Jason Hellmann,[1] Brian E. Sansbury,[1] Candice R. Holden,[2] Yunan Tang,[2] Blenda Wong,[1] Marcin Wysoczynski,[2] Jorge Rodriguez,[3] Aruni Bhatnagar,[2] Bradford G. Hill,[2] and Matthew Spite[1]

CCR7 Maintains Nonresolving Lymph Node and Adipose Inflammation in Obesity

Diabetes 2016;65:2268–2281 | DOI: 10.2337/db15-1689

OBESITY STUDIES

Accumulation of immune cells in adipose tissue promotes insulin resistance in obesity. Although innate and adaptive immune cells contribute to adipose inflammation, the processes that sustain these interactions are incompletely understood. Here we show that obesity promotes the accumulation of CD11c$^+$ adipose tissue immune cells that express C-C chemokine receptor 7 (CCR7) in mice and humans, and that CCR7 contributes to chronic inflammation and insulin resistance. We identified that CCR7$^+$ macrophages and dendritic cells accumulate in adipose tissue in close proximity to lymph nodes (LNs) (i.e., perinodal) and visceral adipose. Consistent with the role of CCR7 in regulating the migration of immune cells to LNs, obesity promoted the accumulation of CD11c$^+$ cells in LNs, which was prevented by global or hematopoietic deficiency of *Ccr7*. Obese *Ccr7*$^{-/-}$ mice had reduced accumulation of CD8$^+$ T cells, B cells, and macrophages in adipose tissue, which was associated with reduced inflammatory signaling. This reduction in maladaptive inflammation translated to increased insulin signaling and improved glucose tolerance in obesity. Therapeutic administration of an anti-CCR7 antibody phenocopied the effects of genetic *Ccr7* deficiency in mice with established obesity. These results suggest that CCR7 plays a causal role in maintaining innate and adaptive immunity in obesity.

Obesity is a strong risk factor for the development of type 2 diabetes as well as cardiovascular disease, nonalcoholic fatty liver disease, and cancer (1). While an increase in adiposity induces pleiotropic changes in metabolism, studies of rodent models of obesity have shown that the development of insulin resistance is in part caused by chronic inflammation (1,2). In obese humans, increased white blood cell count and serum concentrations of inflammatory mediators (e.g., C-reactive protein) are associated with insulin resistance as well (1). During obesity, hypertrophic changes in adipocytes are accompanied by accumulation in tissue of both adaptive and innate immune cells, including macrophages, dendritic cells (DCs), neutrophils, B cells, CD4$^+$ T helper cells, and CD8$^+$ cytotoxic T cells, and it has been found that the accumulation of these cells in the adipose tissue contributes significantly to obesity-induced metabolic derangements (1,3–7). The infiltration of adipose tissue by immune cells in obesity is reminiscent of an acute pathogen challenge; unlike the response of a host to infection, however, inflammation in obesity does not resolve appropriately, and it establishes a perpetual host response that is maintained by both innate and adaptive immune cells (8,9).

The accumulation of adipose tissue macrophages (ATMs) in obesity impairs metabolism, in part because of the production of inflammatory cytokines (e.g., tumor necrosis factor [TNF]-α) that directly perturb insulin signaling (1,10,11). Like DCs, ATMs also function as antigen-presenting cells (APCs); they express the major histocompatibility complex II (MHCII) and costimulatory molecules (CD40 and CD80), and they are sufficient to induce T-cell proliferation (12–14). Obesity also promotes humoral immunity associated with an increase in B-cell-dependent autoantibody production, suggesting that inflammation in obesity is triggered in part by endogenous antigens (4,15). Despite extensive evidence supporting a role for innate and adaptive immunity in metabolic

[1]Center for Experimental Therapeutics and Reperfusion Injury, Department of Anesthesiology, Perioperative and Pain Medicine, Brigham and Women's Hospital and Harvard Medical School, Harvard Institutes of Medicine, Boston, MA
[2]Diabetes and Obesity Center, Institute of Molecular Cardiology, University of Louisville School of Medicine, Louisville, KY
[3]Department of Surgery, University of Louisville School of Medicine, Louisville, KY
Corresponding author: Matthew Spite, mspite@bwh.harvard.edu.

Received 10 December 2015 and accepted 27 April 2016.
This article contains Supplementary Data online at http://diabetes.diabetesjournals.org/lookup/suppl/doi:10.2337/db15-1689/-/DC1.

complications of obesity, the processes that sustain these interactions are incompletely understood.

Recent evidence indicates that in both obese rodents and humans, the abundance of C-C chemokine receptor 7 (CCR7) is increased in ATMs, particularly those that are enriched in lipids and have assumed a proinflammatory M1 phenotype (16–19). CCR7 plays a critical role in host defense by facilitating innate and adaptive immune cell interactions. It is expressed on mature DCs and is required for their migration to lymph nodes (LNs) to present antigen to T cells (20). Activation of CCR7 by its ligands, CCL19 and CCL21, also facilitates antigen uptake by DCs and T-cell proliferation and survival (20,21). Although such activation of CCR7 is protective in the context of pathogen exposure, its activation in several types of cancer and atherosclerosis might be a maladaptive response (22–26). Here we provide evidence that CCR7 maintains adipose tissue and LN inflammation, revealing a previously undescribed link between innate and adaptive immunity in obesity.

RESEARCH DESIGN AND METHODS

Animals and Diets

Male C57BL/6J (wild type [WT]), B6.129P2(C)-*Ccr7*^{tm1Rfor}/J (*Ccr7*$^{-/-}$), B6.SJL-*Ptprc*^{a}*Pepc*^{b}/BoyJ (*CD45.1*), and C57BL/6-Tg(ACTB-EGFP)131Osb/LeySopJ (*GFP*$^{+}$) mice were purchased from the Jackson Laboratory (Bar Harbor, ME) at 4–10 weeks of age. For diet-induced obesity studies, 8- to 10-week-old mice were fed either a low-fat diet (LFD) (10% kilocalories from fat; D12450B formula; Research Diets, Inc.) or a high-fat diet (HFD) (60% kilocalories from fat; D12492 formula), which was maintained for up to an additional 16 weeks unless otherwise indicated. Animals were housed in a 12-h light/12-h dark cycle and given water and food ad libitum. Body weight was measured weekly, and all other parameters were evaluated after euthanasia. All animal procedures were approved by the University of Louisville Institutional Animal Care and Use Committee or by the Harvard Medical Area Standing Committee on Animals (protocol no. 05125).

Human Samples

Patients undergoing bariatric surgeries (gastric imbrication and/or Lap-Band) were recruited under an institutional review board–approved (no. 11.0360) study at the University of Louisville Department of Surgery. Inclusion criteria consisted of subjects being 22 to 65 years old. Subjects who were pregnant; currently taking estrogen, testosterone, anti-TNF agents, or Procrit; were not able or not willing to give consent; or had a history of cancer were excluded from the study. Subjects with HbA_{1c} values $\leq$6.4% and no history of diabetes were considered as not having diabetes. Subjects with HbA_{1c} $\geq$6.5% or who were currently being treated for diabetes were considered to have diabetes. On the day of surgery, visceral and subcutaneous adipose tissues were harvested at the site of surgical incision and immediately placed in Tyrode's solution. Samples were immediately placed on ice and processed for flow cytometry, as described below. The baseline characteristics of the cohort are shown in Supplementary Table 1.

Bone Marrow Transplantation

At 5 weeks of age, recipient male WT CD45.1 mice (B6.SJL-*Ptprc*^{a}*Pepc*^{b}/BoyJ) were conditioned with 950 cGy total-body irradiation from a cesium source (γ-cell 40; Nordion, Ontario, Canada). Bone marrow (BM) was isolated from the tibiae and femurs of syngenic CD45.2 C57BL/6J and CD45.2 *Ccr7*$^{-/-}$ donor male mice (10–12 weeks of age) by flushing the tibiae and femurs with PBS. The BM was resuspended in PBS by gentle aspiration through an 18-gauge needle. The cells were filtered through sterile nylon mesh with 100-μM pores, centrifuged at 1,000 rpm for 10 min at 4°C, and resuspended in PBS. After irradiation (24 h), animals (8 mice/group) underwent transplantation with 0.1 mL PBS containing 1×10^7 BM cells through the retro-orbital plexus using a 27-gauge needle. Five weeks after BM transplant, recipients were characterized for hematopoietic recovery and chimerism by determining the relative percentages of CD45.2 cells in peripheral blood. For this, peripheral blood was obtained through retro-orbital bleeding using a HemaVet 950 (Drew Scientific Inc., Oxford, CT) and was used to count white blood cells; nucleated cells were analyzed by flow cytometry (LSRII) to determine the percentage of CD45.2 cells. Mice with peripheral blood containing $\geq$85% CD45.2^{+} cells were used for further experiments. Only mice meeting these criteria were placed on an HFD for an additional 10 weeks. For enhanced green fluorescent protein (GFP) BM transplant studies, 4- to 5-week-old male C57BL/6J mice were irradiated and repopulated with GFP^{+} BM, as described above. Chimerism was assessed 5 weeks later by flow cytometry. All animals with $\geq$85% GFP^{+} expression in peripheral blood leukocytes were fed either an LFD or an HFD for an additional 12 weeks. At the conclusion of the feeding protocols, inguinal LNs were collected and analyzed by flow cytometry.

Flow Cytometry Analysis

Stromal vascular cell fractions (SVF) were isolated from adipose tissue, as described before (27). Briefly, following euthanasia, perinodal subcutaneous (12-mm punch biopsy surrounding the inguinal LNs) or visceral (epididymal) adipose tissues were isolated from mice fed an LFD or an HFD and the tissue was minced and then digested with collagenase type I (1 mg/mL) in PBS supplemented with 1% FBS for 30 min at 37°C. The digested material was then filtered through a 70-μm mesh cell strainer to achieve a cell suspension, which was followed by centrifugation at 1,000*g* for 10 min at 4°C. The SVF pellet was then incubated with Fc Block for 10 min before staining with fluorescently conjugated primary antibodies. Antimouse antibodies used included Alexa647-CD301 (AbD Serotec, Oxford, U.K.); APC-CCR7 (4B12); PE-Cy7-CD11c; PE-F4/80; APC-e780-CD3; e660-CD4; e605-B220; Alexa 700-MHCII; and PerCP-e710-CD8 (eBioscience, San

Diego, CA). In selected experiments, surface expression of CD64 (phycoerythrin [PE]) was used to identify macrophages, whereas CD8 activation was assessed by the expression of CD62L (PE-Cy7) and CD44 (APC) (eBioscience). A BD LSRII flow cytometer (BD Biosciences) equipped with FACSDiva software (version 6.0) was used for flow cytometry. Analysis was performed using FlowJo software (version 7.6).

Inguinal LN cells were isolated using a 70-μm mesh cell strainer and a sterile rubber plunger from a 5-mL syringe. Strainers were washed carefully with PBS containing 1% FBS. Cell suspensions were centrifuged at 1,000*g* for 10 min at 4°C, and the supernatant was discarded. Cell pellets were used for flow cytometry analysis using fluorescently conjugated primary antibodies. Antimouse antibodies used included APC-CCR7 (4B12), FITC-CD11b, PE-Cy7-CD11c, e605-B220, PE-F4/80, and Alexa 700-MHCII (eBioscience). In select experiments, CD64 (PE conjugates) was used to identify macrophages (eBioscience).

Peripheral blood leukocyte populations were assessed by flow cytometry. For this, blood was collected via cardiac puncture using EDTA as an anticoagulant. Red blood cell lysis was performed on whole blood (500 μL) using BD Pharm Lyse (BD Biosciences). Samples were centrifuged and resuspended in PBS supplemented with 1% FBS. Samples were then incubated on ice for 10 min with Fc Block before staining with fluorescently conjugated antibodies: APC-e780-CD3, e660-CD4, PerCP-e710-CD8, e450-Ly6C, and APC-CCR7 (4B12) (eBioscience). Samples were analyzed by flow cytometry as described above.

For isolation of human adipose tissue SVFs, samples were weighed, minced, and incubated with collagenase type I (1 mg/mL) in isotonic Tyrode's solution at 37°C for 30 min. Samples were passed through a 70-μm mesh cell strainer and centrifuged at 1,000*g* for 10 min. Cell pellets were preincubated with antihuman Fc Block for 10 min on ice. Antihuman primary fluorescent antibodies against CD11b (PerCP-e710), CD11c (fluorescein isothiocyanate [FITC]), and CCR7 (APC; 3D12) (eBioscience) were incubated with the SVF for 30 min on ice. Samples were washed twice with PBS supplemented with 1% FBS and analyzed as described above.

FITC-Ovalbumin LN Tracking

WT or *Ccr7*$^{-/-}$ mice fed an HFD for 12 weeks were anesthetized and the bilateral epididymal fat pads were externalized through a small abdominal incision using aseptic surgical procedures. Fat pads were directly injected with FITC-ovalbumin (OVA) (150 μg/50 μL) using a 29-gauge insulin syringe. Epididymal fat pads were returned to the visceral cavity (28) and the incision was closed using cyanoacrylate adhesive (Vetbond; 3M). After 24 h, animals were euthanized and cell suspensions were prepared from LNs, as described above, before analysis by flow cytometry.

Body Composition and Calorimetry

The body composition of mice was measured using DEXA (PIXImus II; Lunar, Madison, WI) after 16 weeks of LFD or HFD feeding. Additionally, during the 15th week of either LFD or HFD feeding, oxygen consumption (V_{O_2}), carbon dioxide production (V_{CO_2}), and food intake were monitored over a 24-h period using a PhenoMaster system (TSE Systems, Bad Homburg, Germany). Measurements collected during the dark cycle were averaged and used for statistical analysis.

Biochemical Analyses

Whole blood was collected by cardiac puncture using EDTA as the anticoagulant, and plasma was prepared. Total plasma albumin, triglycerides, cholesterol, LDL, HDL, alanine aminotransferase and aspartate aminotransferase concentrations were measured using commercially available assay reagents, as described before (27). Assays were performed using a Cobas Mira Plus 5600 Autoanalyzer (Roche, Indianapolis, IN). Plasma insulin (Mercodia, Uppsala, Sweden) and MCP-1 (Abcam, Cambridge, MA) concentrations were measured by ELISA, and fluorescence was detected using a multimode Synergy microplate reader (BioTek Instruments, Winooski, VT). Immunoglobulin isotypes were analyzed in plasma using a Rapid Mouse Ig Isotyping Array (RayBiotech, Norcross, GA).

In Vitro Macrophage Experiments

Murine macrophages (RAW 264.7; American Type Culture Collection) were plated onto 6-well culture plates in DMEM supplemented with 10% FBS and 1% penicillin/streptomycin and were allowed to grow to 90% confluence. Cells were treated with BSA conjugated to palmitic acid (PA; 6:1 PA-to-BSA ratio; 500-μM final concentration) or equimolar BSA alone for 6 h. Macrophages were then either removed for flow cytometry analysis of CCR7 surface expression, or processed for quantitative RT-PCR (as described below) to determine mRNA expression of *Ccr7* and *Tnfα*.

RT-PCR Analysis and Immunoblotting

For quantitative RT-PCR, RNA was isolated from tissues using an RNeasy Lipid Tissue Kit, whereas an RNeasy Mini Kit (Qiagen, Germantown, MD) was used for in vitro experiments, according to the manufacturer's protocol. DNA polymerization was performed using avian myeloblastosis virus reverse transcriptase (Promega, Madison, WI). Real-time amplification was performed using SYBR Green PerfeCTa with ROX Master Mix (Quanta Biosystems) using a 7900HT Fast Real-Time PCR System (Applied Biosystems, Foster City, CA). Commercially available primers were used for targeted analysis of *Ccr7*, *Ccl19*, *Ccl21*, *Emr1* (F4/80), *Itgax* (CD11c), *Tnfα*, *Ccl2*, and *Hprt* (SA Biosciences). Relative expression was calculated by the $2^{-\Delta\Delta C}{}_T$ method and normalized to endogenous *Hprt* levels.

To assess tissue inflammation and insulin signaling, animals were treated with either 100 μL of Humulin-R (1.5 U/kg; Eli Lilly, Indianapolis, IN) or saline by intraperitoneal injection 15 min before euthanasia. Density of insulin receptor subunit β in liver and skeletal muscle was measured by immunoblotting, whereas AKT phosphorylation status

was assessed in epididymal adipose tissue and skeletal muscle lysates that were prepared using standard procedures. Samples were prepared for SDS-PAGE, transblotted, and probed for insulin receptor β subunit (EMD Millipore, Billerica, MA), phospho-AKT (Ser473), total AKT, and GAPDH (Cell Signaling Technology, Beverly, MA). For tissue inflammation, phosphorylated IκBα (Ser32) and total IκBα (Cell Signaling Technology) were probed. Immunoblots were developed using Luminata Forte Western HRP Substrate (Millipore) and scanned for luminescence using a Typhoon 9400 variable mode imager (GE Healthcare, Chalfont St. Giles, U.K.) or a Kodak M35A X-OMAT processor (Rochester, NY). Image Quant TL software (GE Healthcare) or ImageJ software was used for densitometry analysis.

Glucose Tolerance Tests

Following 6 h of fasting, glucose tolerance tests were performed by intraperitoneal injection of D-glucose (1 mg/g) in sterile saline. Following a tail snip, glucose concentrations were monitored at indicated times using an Aviva Accu-Chek glucometer.

Immunohistochemistry

Hematoxylin-eosin staining was performed following standard procedures to identify crown-like structures in adipose tissue sections that had been fixed in formalin and embedded in paraffin. Crown-like structures in at least five random fields per animal were quantified by a blinded observer. Additionally, Nikon's NIS-Elements Basic Research software was used to measure the area of ~1,000 adipocytes in five random fields per animal from isolated epididymal fat pads. Adipocyte size measurements are expressed as an overall average per animal and are represented in a frequency distribution graph.

For LN immunohistochemistry, LNs were fixed in formalin, embedded in paraffin, and sectioned. After retrieving antigen in deparaffinized sections, samples were blocked with Rodent Block M Blocking Reagent (Biocare, Concord, CA) for 1 h at room temperature and incubated with primary antibody rat antimouse F4/80 (1:50; AbD Serotec) overnight at 4°C. After washing with Tris-buffered saline, slides were incubated with a secondary goat antirat IgG:horseradish peroxidase (AbD Serotec) for 1 h at room temperature. Samples were subsequently developed using a DAB Substrate Kit (Vector Laboratories, Burlingame, CA). Sections were counterstained with hematoxylin, dehydrated, mounted, coverslipped, and photographed using light microscopy. Adjacent sections that underwent same procedure but without the primary antibody were considered negative controls.

Anti-CCR7 Antibody Treatment

To assess the effects of CCR7 blockade, obese WT mice were treated with a monoclonal anti-CCR7 antibody (4B12; eBioscience) (3 μg/g body weight in 500 μL sterile saline; intraperitoneal) or IgG2a isotype control (EBR2; eBioscience) 3 times per week for 6 weeks, starting 6 weeks after the initiation of the HFD (29,30). Mice were maintained on the HFD and weighed weekly. After 12 weeks of HFD feeding, glucose tolerance was measured as described above.

Statistical Analysis

Data are expressed as means ± SEM. Multiple group comparisons were made using one-way or two-way ANOVA, where appropriate, followed by Bonferroni or Tukey tests. For direct comparisons, an unpaired two-tailed Student *t* test was used. $P < 0.05$ was considered significant in all cases.

RESULTS

Obesity Promotes the Accumulation of CCR7$^+$ Innate Immune Cells in Adipose Tissue of Mice and Humans

To examine the role of CCR7 in obesity, we first assessed the infiltration of macrophages into visceral adipose tissue (VAT) in WT mice fed an LFD or an HFD. Flow cytometry analysis of the SVF revealed a prominent F4/80$^+$CD64$^+$ (FcγR1) cell population (31) (Fig. 1*A*). These macrophages were significantly increased by the HFD at both 10 and 16 weeks of feeding (Fig. 1*B*). Nearly 50% of these macrophages expressed CD11c, which is an inflammatory ATM population that contributes to metabolic derangements in obesity (32) (Fig. 1*C*). A subset of these F4/80$^+$CD11c$^+$ macrophages expressed CCR7 (Fig. 1*D* and *E*); expression of CCR7 was not observed on peripheral blood monocytes (Ly6c^{hi}; data not shown), indicating that CCR7 was upregulated in ATMs in adipose tissue. Consistent with the increased surface expression of CCR7 on ATMs, the HFD increased *Ccr7* mRNA expression in VAT (Fig. 1*F*), whereas obesity did not affect the expression of CCR7 ligands *Ccl19* or *Ccl21* in adipose tissue at this time point (Supplementary Fig. 1*A*). As previously reported (33), obesity also significantly increased the accumulation of CD11c^{hi}B220$^-$ DCs (Fig. 1*G*). These cells increased significantly by 10 weeks but subsequently decreased after 16 weeks of the HFD. They expressed CCR7, although when considering the total amount of CCR7$^+$ DCs, no clear relationship with obesity emerged, potentially because of steady-state emigration from the tissue. By contrast, adipose CD11c^{low}B220$^+$ plasmacytoid DCs were not affected by obesity (Supplementary Fig. 1*B*). We also assessed the expression of CCR7 on T cells in VAT and peripheral blood. As observed with ATMs and DCs, CCR7 was expressed on CD3$^+$CD4$^+$ and CD3$^+$CD8$^+$ T cells in VAT. Unlike the clear diet-induced increase in the accumulation of CCR7$^+$ ATMs, CCR7$^+$CD8$^+$ T cells were not affected by obesity and CCR7$^+$CD4$^+$ T cells decreased with obesity (Fig. 1*H*). CCR7 was expressed on T cells circulating in the peripheral blood (Supplementary Fig. 1*C*), although the relative proportion of these CCR7$^+$ cells was not significantly affected by obesity.

We next examined whether CCR7$^+$ ATMs accumulate in other adipose tissue depots during obesity. For this we isolated subcutaneous adipose tissue in close proximity to inguinal LNs (denoted as perinodal adipose tissue [PAT]) because recent studies have shown that immune cells

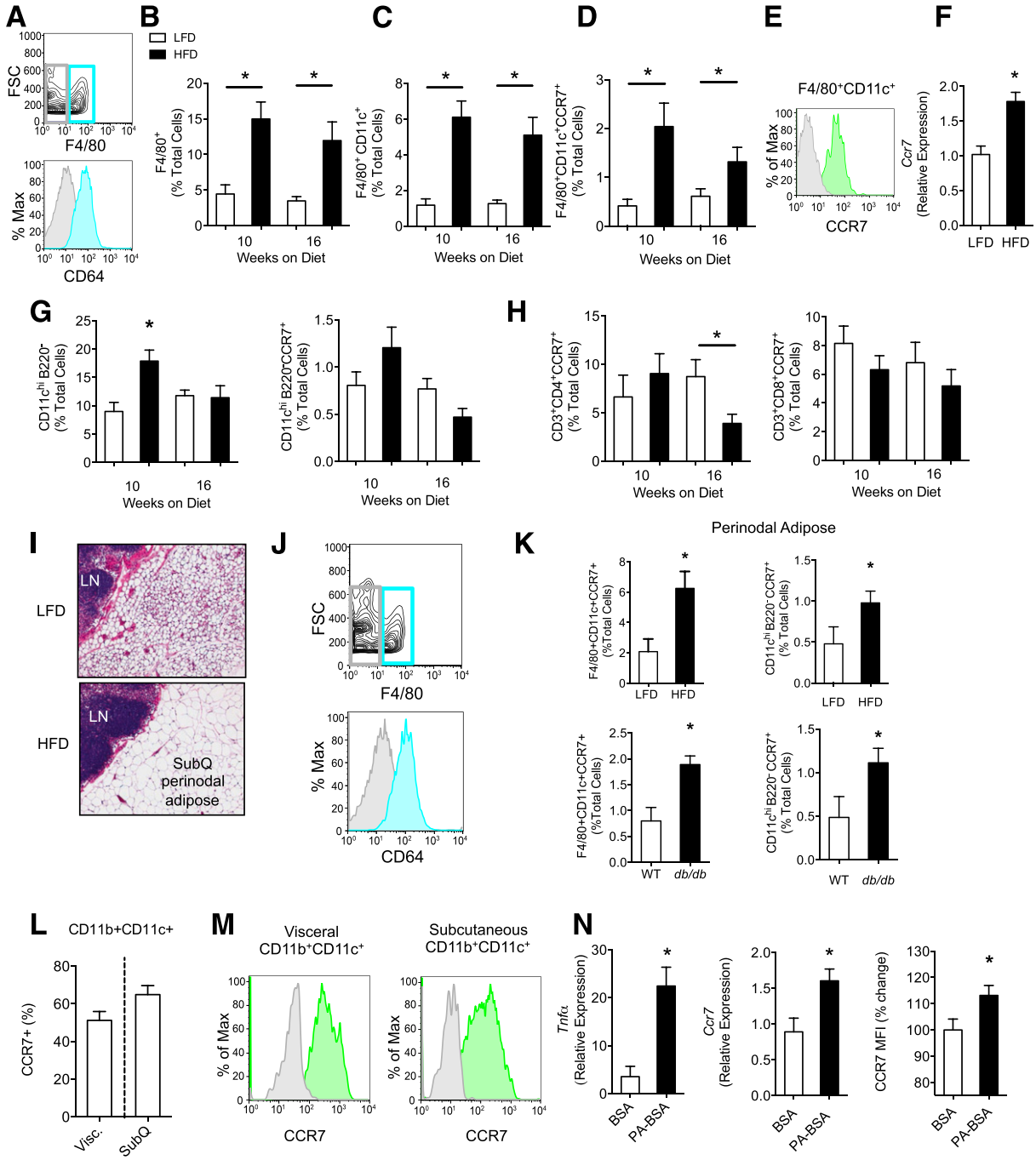

Figure 1—CCR7$^+$ macrophages and DCs accumulate in adipose tissue of obese mice and humans. *A*: Flow cytometry analysis of CD64$^+$F4/80$^+$ macrophages in VAT of mice fed an HFD for 10 weeks. FSC, forward scatter. *B–D*: Time-dependent accumulation of F4/80$^+$ (*B*), F4/80$^+$CD11c$^+$ (*C*) and F4/80$^+$CD11c$^+$CCR7$^+$ (*D*) macrophages in VAT of WT mice fed an LFD or an HFD for 10 or 16 weeks (n = 9 or 10 per group per time point). *E*: Representative flow cytometry analysis of CCR7 surface expression on F4/80$^+$CD11c$^+$ adipose tissue macrophages. *F*: Expression of *Ccr7* mRNA in adipose tissue of WT mice (n = 4) fed an LFD or HFD for 16 weeks. *G*: Quantification of CD11c^{hi}B220$^-$ and CD11c^{hi}B220$^-$CCR7$^+$ DCs in VAT of mice fed an LFD or an HFD for 10 or 16 weeks (n = 9 or 10 per group per time point). *H*: Quantification of CCR7$^+$ T cells in VAT of mice fed an LFD or an HFD for 10 or 16 weeks (n = 9 or 10 per group per time point). *I*: Representative histology (hematoxylin-eosin; original magnification ×10) of PAT surrounding inguinal LNs of WT mice fed an LFD or an HFD for 10 weeks. *J*: Representative flow cytometry analysis of F4/80$^+$CD64$^+$ macrophages in PAT of obese WT mice. *K*: Quantification of F4/80$^+$CD11c$^+$CCR7$^+$ macrophages and CD11c^{hi}B220$^-$CCR7$^+$ DCs in subcutaneous PAT of WT mice fed an LFD or an HFD for 10 weeks or WT mice and leptin receptor–deficient mice (*db/db*) fed normal chow (n = 4 or 5 per group). *L* and *M*: Quantification of CCR7$^+$CD11b$^+$CD11c$^+$ cells in visceral (Visc.) or subcutaneous (SubQ) adipose tissue depots (n = 12 per depot) of obese humans undergoing bariatric surgery (*L*), with representative flow cytometry histograms of CCR7 expression on CD11b$^+$CD11c$^+$ cells shown (*M*). *N*: mRNA expression of *Tnfα* and *Ccr7* in murine macrophages stimulated for 6 h with BSA control or PA-BSA conjugates (n = 8–10 per group). Surface expression of CCR7 in macrophages stimulated with BSA or PA-BSA, presented as percentage change in mean fluorescence intensity (MFI), is shown in the panel on the right. Data are mean ± SEM. *P < 0.05.

traffic through PAT during acute inflammation (34,35). Histological analysis revealed a marked transition from numerous small adipocytes to large white adipocytes in PAT, a change similar to that which occurs in VAT (Fig. 1*I*). Flow cytometry analysis showed that F4/80$^+$CD64$^+$ macrophages were present in isolated PAT (Fig. 1*J*) and that the proportion of F4/80$^+$CD11c$^+$CCR7$^+$ ATMs increased when the mice were fed an HFD (Fig. 1*K*). We also observed a significant increase in CD11c^{hi}B220$^-$CCR7$^+$ DCs in PAT with HFD feeding (Fig. 1*K*, top right panel). Similar accumulation of CCR7$^+$ ATMs and DCs in PAT was observed in leptin receptor–deficient mice (*db/db*), a genetic model of obesity and type 2 diabetes (Fig. 1*K*, bottom panels).

To determine whether CCR7 is expressed on immune cells in human adipose tissue, we obtained VAT and subcutaneous adipose tissue from obese individuals (BMI >30 kg/m^2) undergoing bariatric surgery procedures (i.e., gastric imbrication or Lap-Band). Baseline clinical characteristics of this cohort are shown in Supplementary Table 1. Both VAT and subcutaneous adipose tissue depots contained abundant CD11b$^+$CD11c$^+$ cells that expressed CCR7 (Fig. 1*L*). Representative flow cytometry histograms of CCR7 expression on these cells from one patient are shown in Fig. 1*M*; histograms for each individual bariatric surgery patient are shown in Supplementary Fig. 2. Collectively, these results indicate that CCR7$^+$ innate immune cells are associated with adipose tissue inflammation in obese mice and humans.

Saturated Fatty Acids Increase CCR7 Expression in Macrophages

It is well documented that saturated fatty acids, which are a primary component of an HFD, activate stress and inflammatory signaling pathways in macrophages (1,36). Moreover, *Ccr7* is expressed in lipid-laden ATMs (17); hence fatty acids might be involved in upregulating CCR7. To test the role of saturated fatty acids as a potential stimulus for CCR7 expression, we stimulated murine macrophages with PA and measured the expression of *Ccr7*. We found that PA increased the production of the inflammatory cytokine *Tnfα*, as well as *Ccr7* (Fig. 1*N*). In addition to mRNA, PA also significantly enhanced CCR7 surface expression on macrophages. These data suggest that during obesity, elevated saturated fatty acids might increase *Ccr7* expression in macrophages.

Obesity Promotes Macrophage and DC Accumulation in LNs in a CCR7-Dependent Manner

Given both the well-defined role of CCR7 in promoting APC migration to LNs (20) and that we identified CCR7$^+$ ATMs and DCs in PAT surrounding LNs, we next asked whether obesity promotes their accumulation in LNs. Histological analysis of LNs isolated from WT mice showed an obesity-induced accumulation of F4/80$^+$ macrophages in the paracortical region, which was prevented by *Ccr7* deficiency (Fig. 2*A* and *B*). Using flow cytometry analysis of cell suspensions isolated from LNs, we found that F4/80$^+$ LN macrophages expressed CD64 (Fig. 2*C*). HFD feeding increased CCR7$^+$F4/80$^+$ macrophages and CD11c^{hi}B220$^-$ DCs in LNs (Fig. 2*D*). Accordingly, the HFD significantly increased *Ccr7* mRNA expression in LNs (Fig. 2*D*). We also observed that the HFD increased the expression of the proinflammatory cytokine *Tnfα* in LNs (Fig. 2*D*), similar to what occurs in adipose tissue during obesity. Consistent with the role of CCR7 in promoting the migration of immune cells to LNs, the accumulation of both macrophages (CD11c$^+$MHCII$^+$F4/80$^+$) and DCs (CD11c^{hi}B220$^-$) was significantly blunted in obese *Ccr7*-deficient mice (Fig. 2*E*). By contrast, we observed the opposite trend in the local PAT, where both cell populations increased in obese *Ccr7*-deficient mice (Fig. 2*F*). Unlike the CD11c^{hi}B220$^-$ DCs, plasmacytoid DCs decreased in both PAT and LNs during obesity (Supplementary Fig. 1D and *E*). These collective results suggest that CCR7 promotes the migration of macrophages and DCs to LNs during obesity and that loss of *Ccr7* increases their accumulation in local PAT, perhaps as a result of impaired migration out of the PAT.

It is well documented that CCR7 promotes the migration of DCs to LNs (20). To determine whether macrophages are recruited to LNs during obesity, we carried out BM transplantation (BMT) experiments in which BM from mice expressing GFP was transplanted into WT recipient mice. Recipient mice were then placed on an LFD or HFD for 12 weeks (Fig. 3*A*). Reconstitution of WT recipient mice with hematopoietic cells from GFP$^+$ mice revealed the abundant accumulation of GFP$^+$F4/80$^+$ macrophages in LNs (Fig. 3*B*). A subpopulation of these cells expressed CD11c and MHCII, and the HFD significantly increased the numbers of these cells in the LNs (Fig. 3*B*). Also, the HFD significantly increased the accumulation of GFP$^+$CCR7$^+$CD11c$^+$F4/80$^+$MHCII$^+$ macrophages in LNs. These results suggest that obesity increases CCR7$^+$ macrophage recruitment to LNs. Global deficiency of *Ccr7* has been documented to perturb LN architecture and the quantity of immune cells in tissue (20,21). To rule out such phenotypic alterations in the reduction of CCR7$^+$ macrophages observed in the LNs of obese *Ccr7*-deficient mice (see Fig. 2), either WT (CD45.2) or *Ccr7*-deficient (CD45.2) BM was transplanted into WT (CD45.1) recipients, and the mice were fed an HFD for 10 weeks (Fig. 3*C*). Chimerism was determined by assessing the percentage of CD45.2 leukocytes in the peripheral blood, which was consistently $>85\%$ (Fig. 3*D*). In WT mice transplanted with *Ccr7*-deficient BM, a significant decrease in the accumulation of F4/80$^+$CD11c$^+$MHCII$^+$ cells in LNs was observed compared with mice transplanted with WT BM (Fig. 3*E*).

To directly test whether ATMs can traffic to LNs in a CCR7-dependent manner, we assessed the trafficking of ATMs exposed to a model antigen, OVA. For this, WT or *Ccr7*-deficient mice were fed an HFD for 12 weeks, and their epididymal fat pads were surgically extruded through

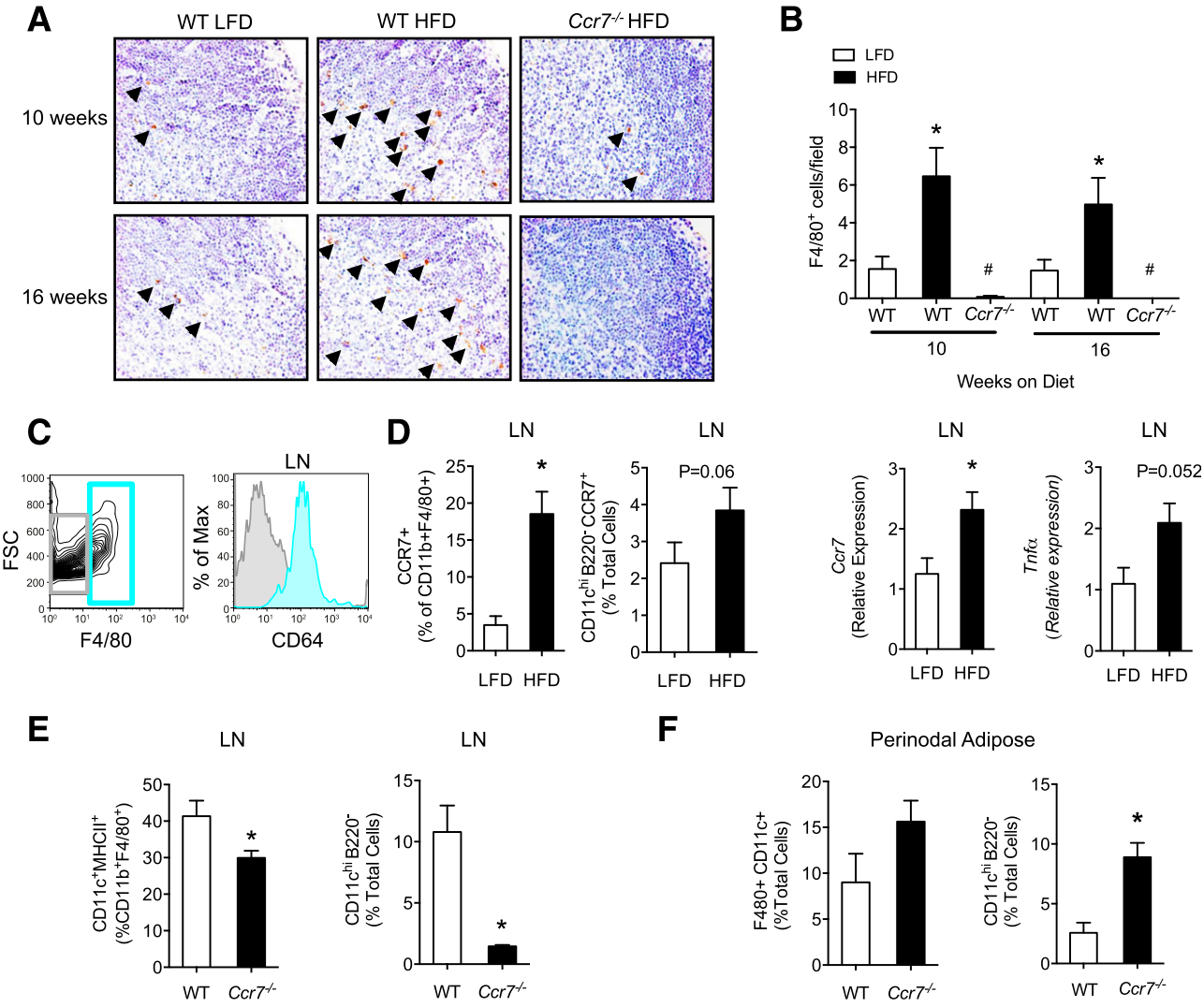

Figure 2—Obesity promotes macrophage and DC accumulation in LNs in a CCR7-dependent manner. *A*: Representative immunohistochemical analysis of F4/80$^+$ cells (indicated by arrowheads; original magnification ×40) in LNs isolated from WT or *Ccr7*-deficient mice fed an LFD or HFD for 10 or 16 weeks; quantification is shown in *B*; n = 3–9 per group per time point averaged across five random fields per animal. *$P < 0.05$, WT LFD vs. HFD groups; #$P < 0.05$, compared with the WT HFD group. *C*: Representative flow cytometry analysis of F4/80$^+$CD64$^+$ macrophages in LNs of mice fed an HFD for 10 weeks. FSC, forward scatter. *D*: Quantification of CCR7$^+$ macrophages and DCs in LNs of WT mice fed an LFD or an HFD for 10 weeks. Panels on the right show the expression of *Ccr7* and *Tnfα* mRNA in LNs. *E* and *F*: Quantification of macrophages and DCs in LNs and PAT of WT or *Ccr7*-deficient mice fed an HFD for 10 weeks. n = 5–12 per group (*D*–*F*). Data are mean ± SEM. *$P < 0.05$.

the abdomen and directly injected with FITC-OVA (see RESEARCH DESIGN AND METHODS). The fat pads were placed back into the cavity and after 24 h, and OVA$^+$ macrophages in LNs were quantified. We found that in WT mice fed an HFD, LN macrophages (CD45$^+$F4/80$^+$) were positive for FITC-OVA, whereas LNs from *Ccr7*-deficient mice were largely devoid of these cells (Fig. 3*F*), indicating that ATMs were recruited to the LNs in a CCR7-dependent manner.

CCR7 Promotes Adipose Tissue Inflammation in Obesity

Our results demonstrate that CCR7 is upregulated in adipose tissue and that CCR7 promotes the migration of macrophages and DCs to LNs during obesity. Because previous studies demonstrated that both ATMs and DCs can activate adaptive immune cells (13,33), we hypothesized that by blocking CCR7-dependent recruitment of these cells to LNs, the subsequent recirculation of activated T cells and B cells to adipose tissue should be blunted. Indeed, obesity increased the quantity of CD3$^+$CD8$^+$ cells in the adipose tissue of WT mice, and this diet-dependent increase was absent in *Ccr7*-deficient mice (Fig. 4*A*). We note that the relative proportion of activated (CD62L^{low}CD44$^+$) CD8$^+$ T cells was not different between WT and *Ccr7*-deficient mice (Supplementary Fig. 3). In contrast to CD8$^+$ T cells, diet-induced obesity decreased the numbers of CD3$^+$CD4$^+$ T cells in the adipose tissue

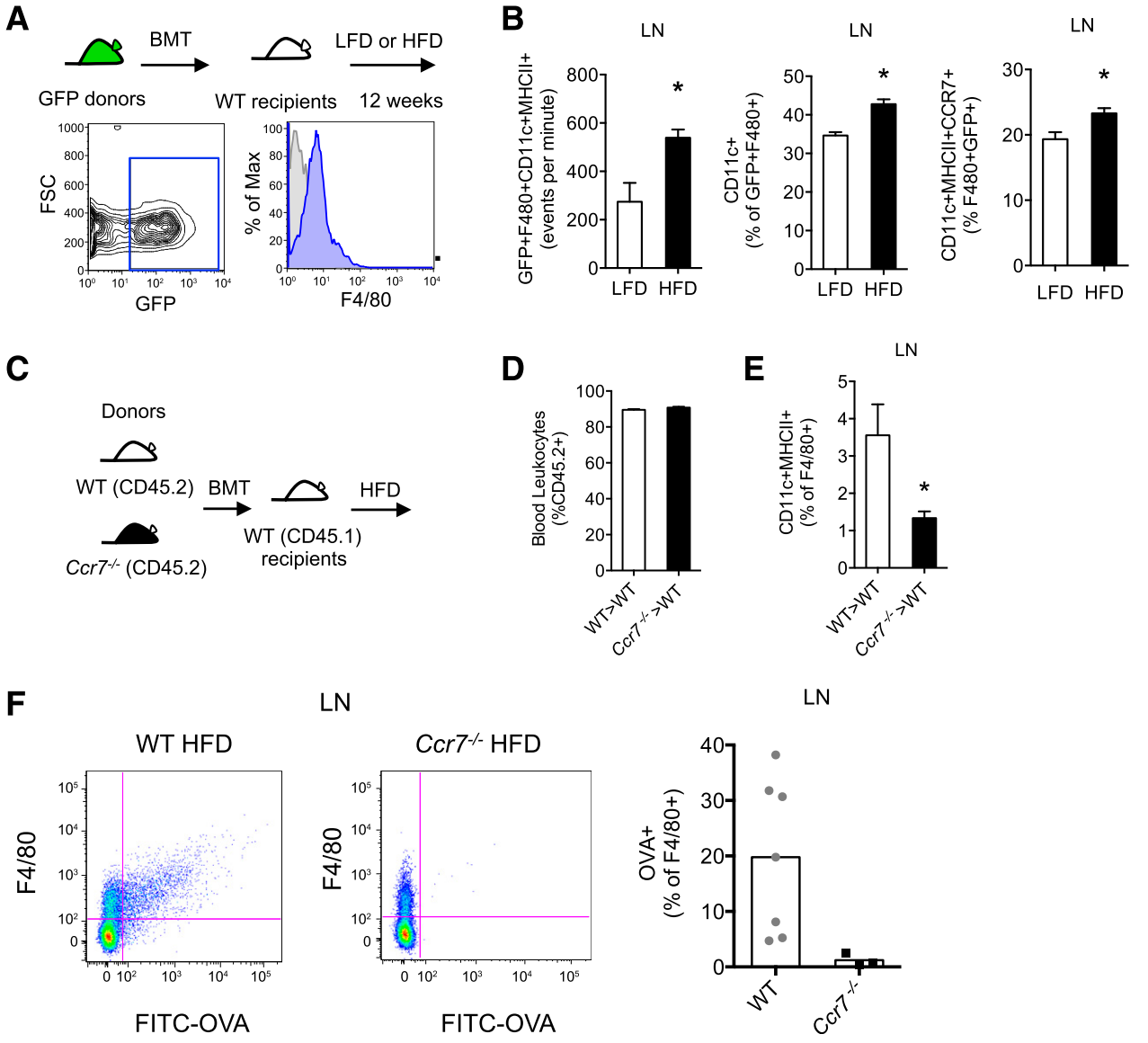

Figure 3—CCR7 regulates trafficking of adipose tissue macrophages to LNs during obesity. *A*: Schematic of BMT of GFP$^+$ cells into WT recipients, which were fed an LFD or an HFD for 12 weeks after transplantation (top). Representative flow cytometry analysis of GFP$^+$F4/80$^+$ macrophages isolated from LNs (bottom). FSC, forward scatter. *B*: Levels of GFP$^+$ macrophage subsets in LNs of mice fed an LFD or an HFD, as determined by flow cytometry (n = 4 per group). *C*: Schematic of the BMT from WT or *Ccr7*-deficient mice (CD45.2) into WT (CD45.1) recipients, followed by HFD feeding for 10 weeks. *D*: Levels of CD45.2$^+$ peripheral blood leukocytes of WT (CD45.1) mice transplanted with WT (CD45.2) or *Ccr7*-deficient (CD45.2) cells and fed an HFD for 10 weeks (n = 8 per group). *E*: Levels of F4/80$^+$CD11c$^+$MHCII$^+$ macrophages in LNs (n = 8 per group). *F*: Representative flow cytometry dot plots of FITC-OVA$^+$F4/80$^+$ cells (pregated on total CD45$^+$ cells) in LNs of WT or *Ccr7*-deficient mice fed an HFD for 10 weeks and administered FITC-OVA by intraepididymal fat pad injection (n = 3–7 per group). Grouped data are shown in the panel on the right. Data are mean ± SEM. *P < 0.05.

of WT mice at this time point; this decrease was not affected by *Ccr7* deficiency (Fig. 4*B*).

Recent reports have also demonstrated a pathogenic role for B cells in the development of adipose inflammation in obesity (4,7). Obesity increased B220$^+$ B cells in adipose tissue, and this effect was completely reversed by *Ccr7* deficiency (Fig. 4*C*). In addition to the role of B cells in regulating cytokine production by T cells, B cells also contribute to humoral immunity in obesity by increasing the production of autoantibodies (4,7). Indeed, obesity significantly increased plasma concentrations of IgG_1 in WT mice, whereas this increase was completely prevented by *Ccr7* deficiency (Fig. 4*D*).

Because cytotoxic CD8$^+$ T cells precede the infiltration of ATMs during obesity and contribute to monocyte recruitment by producing CCL2 (6), we next evaluated whether ATM accumulation was affected by *Ccr7* deficiency. We observed that obesity profoundly increased (by >60-fold) *Ccl2* expression locally in adipose tissue, whereas this obesity-induced increase was largely blunted

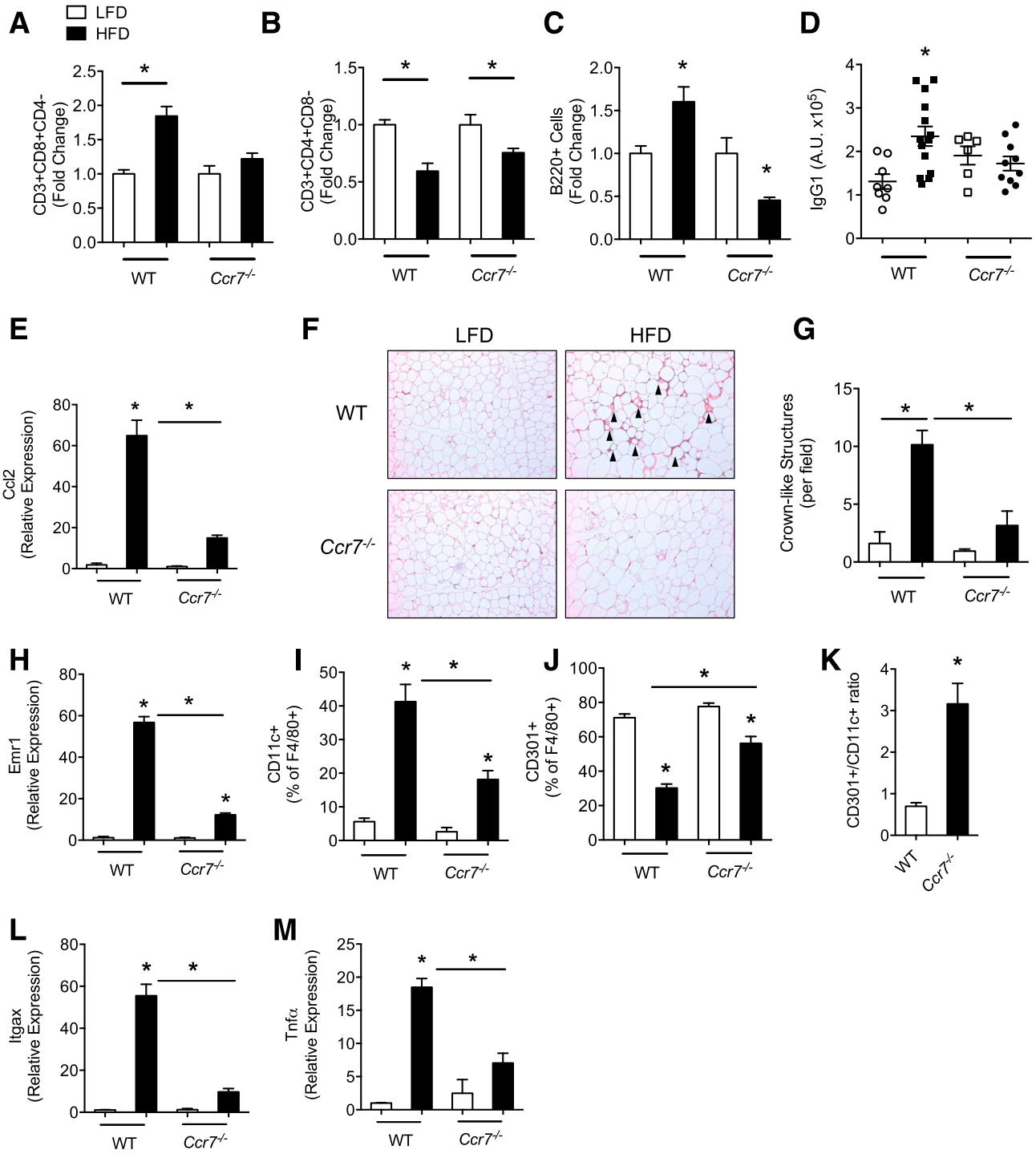

Figure 4—CCR7 promotes adipose tissue inflammation in obese mice. *A–C*: Levels of $CD3^+CD8^+$ T cells, $CD3^+CD4^+$ T cells, and B cells in adipose tissue of WT and *Ccr7*-deficient mice (n = 6–11 per group). *D*: Plasma concentrations of IgG_1 in WT and *Ccr7*-deficient mice fed an LFD or an HFD for 16 weeks (n = 6–14 per group). *E*: mRNA expression of *Ccl2* in adipose tissue of WT and *Ccr7*-deficient mice fed an LFD or an HFD (n = 3 or 4 per group). Arrowheads indicate crown-like structures. *F*: Representative photomicrographs (stained with hematoxylin-eosin) of VAT isolated from WT or *Ccr7*-deficient mice fed an LFD or an HFD for 16 weeks (original magnification ×10). *G*: Quantification of crown-like structures (n = 4 per group, with five random fields per animal). *H*: mRNA expression of *Emr1* (F4/80) in adipose tissue (n = 3 or 4 per group). *I* and *J*: Levels of $CD11c^+$ and $CD301^+$ macrophages ($F4/80^+$) in adipose tissue of WT and *Ccr7*-deficient mice fed an LFD or an HFD for 16 weeks, as determined by flow cytometry (n = 6–11 per group). *K*: Ratio of $CD301^+$ to $CD11c^+$ adipose tissue macrophages (n = 6–11 per group). *L* and *M*: mRNA expression of *Itgax* (CD11c) and *Tnfα* in adipose tissue of WT and *Ccr7*-deficient mice (n = 3 or 4 per group). Data are mean ± SEM. *$P < 0.05$.

in *Ccr7*-deficient mice (Fig. 4*E*). Plasma concentrations of MCP-1 (encoded by *Ccl2*) were not affected by obesity or *Ccr7* deficiency, indicating that loss of *Ccr7* affected local adipose tissue inflammation (Supplementary Fig. 4). Accordingly, there was a significant decrease in the formation of crown-like structures, which are indicative of adipose tissue inflammation (32), in obese *Ccr7*-deficient mice (Fig. 4*F* and *G*). This was further substantiated by decreased expression of *Emr1* (which encodes F4/80) in HFD-fed *Ccr7*-deficient mice compared with WT mice (Fig. 4*H*). Using flow cytometry analysis, we observed a significant reduction in $CD11c^+F4/80^+$ (M1) ATMs in HFD-fed *Ccr7*-deficient mice, whereas the opposite trend was found for $CD301^+F4/80^+$ (M2) ATMs (Fig. 4*I–K*). Consistent with the decrease in $CD11c^+$ macrophages, expression of *Itgax* (CD11c) was substantially reduced in obese *Ccr7*-deficient mice (Fig. 4*L*). The reduction in M1 ATMs was associated with the decreased expression of *Tnfα*, which directly impairs insulin signaling (1,11) (Fig. 4*M*). Collectively, these results suggest that CCR7-dependent migration of innate immune cells to LNs leads to the activation of adaptive immune cells that infiltrate adipose tissue, promote monocyte/macrophage recruitment, and exacerbate inflammatory cytokine production in obesity.

Genetic Deficiency of *Ccr7* Improves Systemic Metabolism in Obesity

Because *Ccr7* deficiency reduced the diet-induced accumulation of both innate and adaptive immune cells in adipose tissue, as well as the production of cytokines that promote insulin resistance (e.g., TNF-α) (10,11), we next sought to determine whether loss of *Ccr7* affects obesity and systemic metabolism. When fed an HFD, weight gain and fat mass in *Ccr7*-deficient mice were similar to those in WT mice (Fig. 5*A* and *B*). The size distribution of adipocytes was also similar between WT and *Ccr7*-deficient mice (Fig. 5*C* and *D*). Obese WT and *Ccr7*-deficient mice had similar blood cholesterol concentrations, food intake, V_{O_2}, and V_{CO_2} (Fig. 5*E* and *F*). No significant differences between obese WT and *Ccr7*-deficient mice were found for heart and spleen weights, liver enzymes (i.e., alanine aminotransferase, aspartate transaminase), plasma triglycerides, or albumin (Supplementary Table 2). However, HFD significantly increased liver weight in WT mice but not *Ccr7*-deficient mice.

As shown in Fig. 5*G*, HFD feeding for 16 weeks significantly increased fasting blood glucose concentrations in WT mice, but *Ccr7* deficiency prevented this increase. Obesity-induced hyperinsulinemia was also drastically reduced in obese *Ccr7*-deficient mice compared with obese WT mice (Fig. 5*G*). Accordingly, the HOMA of insulin resistance was significantly improved in *Ccr7*-deficient mice (Fig. 5*G*), and obese *Ccr7*-deficient mice were more tolerant of glucose than WT mice (Fig. 5*H*). Insulin-stimulated phosphorylation of the downstream effector AKT was significantly blunted in the adipose tissue and skeletal muscle of WT mice fed an HFD compared with their LFD-fed counterparts (Fig. 5*I* and Supplementary Fig. 5*A*). This diet-induced loss of insulin signaling was prevented in *Ccr7*-deficient mice (Fig. 5*I* and Supplementary Fig. 5*A*). Genetic deficiency of *Ccr7* did not affect total levels of the insulin receptor β in skeletal muscle or liver (Supplementary Fig. 5*B* and *C*). Consistent with decreased inflammation and improved insulin signaling, obese *Ccr7*-deficient mice had less phosphorylated IκBα in their adipose tissue (1) (Fig. 5*J*). Collectively, these results indicate that CCR7 contributes to metabolic derangements by promoting adipose tissue inflammation in obesity and that loss of *Ccr7* is sufficient to reduce adipose tissue insulin resistance and systemic glucose intolerance.

Therapeutic Antagonism of CCR7 Improves Glucose Tolerance in Mice With Established Obesity

We also asked whether blockade of CCR7 activity is sufficient to reverse established inflammation and glucose intolerance in obese mice. For this, first we measured blood glucose concentrations on a weekly basis in WT and *Ccr7*-deficient mice fed an HFD and determined that they diverge by 6 weeks after beginning the HFD (data not shown). Then, we treated obese WT mice with an anti-CCR7 antibody or isotype control beginning at 6 weeks of HFD feeding, and we continued treatment for an additional 6 weeks (Fig. 6*A*). We found that treatment with the anti-CCR7 antibody significantly improved glucose tolerance in obese mice despite continued HFD feeding (Fig. 6*B* and *C*). This improvement in glucose tolerance was independent of changes in body weight, as observed with *Ccr7*-deficient mice (Fig. 6*D*). These findings suggest that biologic inhibition of CCR7 could be a feasible approach for attenuating obesity-induced metabolic dysfunction.

DISCUSSION

The results of this study demonstrate that CCR7 perpetuates chronic inflammation in obesity. This role of CCR7 is supported by our observations showing that CCR7 is expressed in innate immune cells (i.e., macrophages and DCs) in adipose tissue of both obese rodents and humans, and that deficiency of *Ccr7* decreases the recruitment of macrophages and DCs to LNs and the subsequent recirculation of adaptive immune cells to adipose tissue. Together, these findings suggest that CCR7 is critical for maintaining maladaptive inflammation and consequent metabolic dysfunction in obesity.

Our observation that *Ccr7* deficiency reduces adipose tissue inflammation is consistent with the known role of this receptor in orchestrating both innate and adaptive immune responses (20,21). Previous studies have shown that by guiding APCs to LNs, CCR7 plays a key role in promoting innate and adaptive immune cell interactions (20). Once activated in LNs, adaptive immune cells recirculate and respond to antigens in affected tissues. Consistent with this role of CCR7, we found that during obesity, CCR7 is expressed on macrophages and DCs in

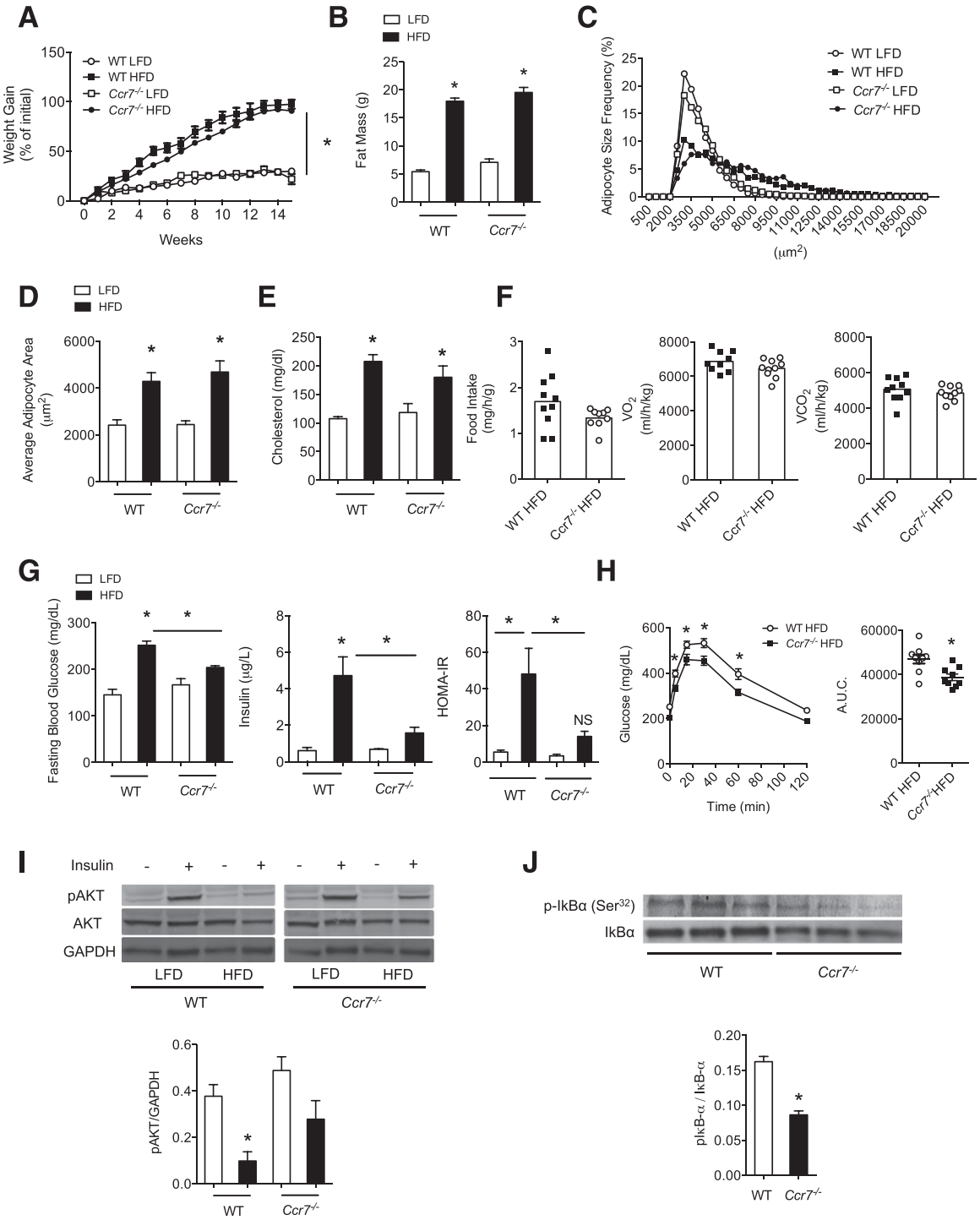

Figure 5—Genetic deficiency of *Ccr7* improves systemic metabolism in obese mice. *A*: Time-dependent changes in body weight of WT or *Ccr7*-deficient mice fed an LFD or an HFD (n = 10–11 per group). *B*: Total body fat mass, as determined by DEXA scan (n = 3 or 4 per group; see RESEARCH DESIGN AND METHODS). *C*: Distribution of adipocytes (based on size) in epididymal fat of WT and *Ccr7*-deficient mice following 16 weeks of feeding (n = 3 or 4 per group, with five random fields per animal). *D*: Average adipocyte area in epididymal fat of WT and *Ccr7*-deficient mice fed an LFD or an HFD for 16 weeks (n = 3 or 4 per group, with five random fields per animal). *E*: Total plasma cholesterol in WT and *Ccr7*-deficient mice fed an LFD or an HFD for 16 weeks (n = 6 per group). *F*: Metabolic cage analysis of food intake, VO_2, and VCO_2 in obese WT and *Ccr7*-deficient mice (n = 10 per group). *G*: Fasting plasma blood glucose and insulin concentrations, and the calculated HOMA of insulin resistance (HOMA-IR) in WT and *Ccr7*-deficient mice fed an LFD or an HFD for 16 weeks (n = 3–10 per group). *H*: Glucose tolerance tests of obese WT and *Ccr7*-deficient mice (n = 3–10 per group); total area under the curve (A.U.C.) analysis is shown in the panel on the right. *I* and *J*: Western blot analysis of insulin-stimulated phosphorylation of AKT (Ser^{473}) and levels of phosphorylated IκBα in epididymal adipose tissue of WT or *Ccr7*-deficient mice fed an LFD or an HFD for 16 weeks. Quantification of band intensity (n = 3–6 per group) is shown in the bottom panels. Data are mean ± SEM. *$P < 0.05$. NS, not significant.

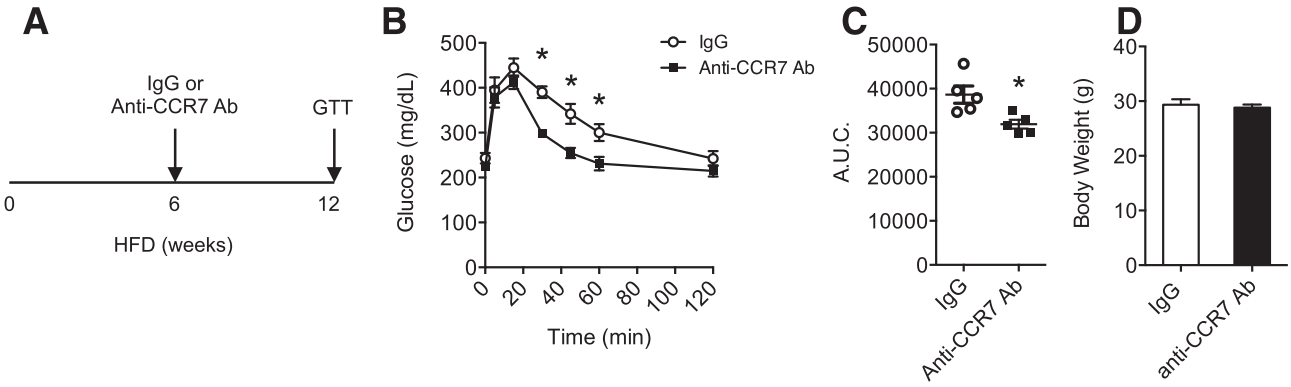

Figure 6—CCR7 blockade improves glucose tolerance in mice with established obesity. *A*: Schematic of the antibody (Ab) treatment protocol in which WT mice fed an HFD for 12 weeks were given intraperitoneally either IgG isotype (control) or an anti-CCR7 monoclonal Ab (3 μg/g body weight in 500 μL sterile saline, three times per week), starting at week 6 (n = 4 or 5 per group). *B*: Glucose tolerance tests of mice treated as described in *A*. *C*: Area under the curve (A.U.C.) obtained from the glucose tolerance tests shown in *B*. *D*: Final body weight of obese mice treated with IgG control or the anti-CCR7 Ab. Data are mean ± SEM. *$P < 0.05$.

adipose tissue and that this is essential for their accumulation in LNs. In addition to DCs, ATMs express MHCII and costimulatory molecules (CD40 and CD80) and are able to interact with T cells and stimulate their proliferation (12,13). The importance of these interactions is highlighted by the observation that in rodent models of obesity, macrophage-specific deletion of MHCII improves systemic metabolism and reduces adipose tissue inflammation (12). In support of the view that CCR7-dependent recruitment of APCs to LNs contributes to systemic inflammation in obesity, *Ccr7* deficiency reduced the accumulation of $CD8^+$ T cells and B cells in adipose tissue and decreased the production of inflammatory mediators that perturb insulin signaling (e.g., TNF-α) (10,11). These changes translated into improved systemic metabolism and are consistent with a report published during the preparation of our article describing a similar pathogenic role of CCR7 in insulin resistance (although the involvement of CCR7 in recruitment of macrophages or DCs to LNs was not investigated) (37).

In addition to adaptive immune cells, we also found that *Ccr7* deficiency blunts the accumulation of M1 ATMs in obesity. Given that CCR7 was not expressed on peripheral blood monocytes, it is unlikely that CCR7 mediates the infiltration of these cells into adipose tissue. A more likely explanation is that the reduction of ATMs is the result of decreased diet-induced accumulation of $CD8^+$ T cells in the adipose tissue of *Ccr7*-deficient mice, since $CD8^+$ T cells have been shown to contribute to the recruitment of monocytes to adipose tissue by producing CCL2 (6). Indeed, both $CD8^+$ T cells and *Ccl2* were significantly lower in the adipose tissue of obese *Ccr7*-deficient mice. We note that there were no clear diet-induced changes in $CCR7^+CD8^+$ T cells, indicating that the reduction in $CD8^+$ T cells in the adipose tissue of obese *Ccr7*-deficient mice was likely indirectly modulated by CCR7 (e.g., decreased T-cell activation by APCs in LNs and subsequent recirculation). However, we cannot conclusively rule out that CCR7 also plays a direct role in the recirculation of adaptive immune cells to adipose tissue. Indeed, CCR7 plays a similar role in recruiting T cells to atherosclerotic lesions (38). Recent studies have documented a pathogenic role for B cells in the development of inflammation in obesity (4,7), similar to the pathogenic role of certain T-lymphocyte subsets in obesity. These B cells activate T cells and produce autoantibodies, and therefore their depletion improves systemic metabolism in obesity (4,7,15). Consistent with this view, our results show that *Ccr7* deficiency decreased HFD-induced infiltration of B cells into adipose tissue and the plasma concentrations of IgG_1 antibodies. Because total IgG isolated from obese mice is sufficient to induce metabolic dysfunction in obesity (4), these results provide additional evidence that CCR7 contributes to obesity-induced metabolic derangements.

We found that diet-induced obesity was associated with a dramatic increase in PAT "whitening." Previous studies showed that long-term mild inflammation enlarges PAT, and "leaky" lymphatics associated with *Prox1* haplosufficiency increases adipose tissue expansion (39,40). Increased lymphatic permeability has been observed in obese diabetic mice, and TNF-α directly stimulates permeability and insulin resistance (11,41). Moreover, immune cell activation increases lipolysis in PAT, and these perinodal adipocytes respond to inflammatory cytokines (40). Indeed, TNF-α stimulates lipolysis (42), and we found that *Tnfα* production in LNs is increased in obesity. We also observed that saturated fatty acids increase *Ccr7* expression in macrophages. Because saturated fatty acids drive macrophage accumulation in adipose tissue and stimulate inflammatory signaling (1,43), it is likely that these fatty acids are a prominent stimulus for increased CCR7 expression in obesity. We found that obesity promotes the accumulation of macrophages and DCs in LNs in a CCR7-dependent manner and that deficiency of *Ccr7* decreased the accumulation of these cells in LNs, with a reciprocal increase in PAT. We therefore posit that macrophages and

DCs in PAT migrate to local LNs in response to elevated amounts of fatty acids and activate adaptive immune cells, which then recirculate and respond to antigens in adipose tissue throughout the body. This is supported by a recent study showing that CCR7 is required for APCs (both DCs and macrophages) to migrate from PAT to local LNs during an acute antigen challenge and that this leads to T-cell recirculation (35). Moreover, given that infection promotes lymphatic leakiness and the deposition of immune cells in adipose tissue (44), our results support the emerging view that there is a dynamic relationship between LN immunity and PAT. Given that the majority of fat in the diet is initially absorbed and transported through the lymphatics via chylomicrons, it is intriguing to speculate that the onset of systemic adipose tissue inflammation in obesity may originate in PAT and/or LNs.

In summary, the results of this study uncover a new role for CCR7 in promoting inflammation and metabolic dysfunction in obesity. We identified $CCR7^+$ innate immune cells in adipose tissue of obese humans and rodents and found that CCR7 promotes the accumulation of macrophages and DCs in LNs during obesity. Genetic deficiency of *Ccr7* is sufficient to disrupt obesity-induced inflammation and insulin resistance, and therapeutic administration of an anti-CCR7 antibody mimicked these effects. Given that CCR7 is currently being tested as a target for the treatment of metastatic cancer (24), these studies could inform the development of novel immunotherapies for treating metabolic disease.

Funding. This work was supported in part by National Institute of General Medical Sciences grant GM103492 (A.B., B.G.H., and M.S.) and by National Heart, Lung, and Blood Institute grant HL106173 (M.S.). J.H. is the recipient of a National Research Service Award from the National Heart, Lung, and Blood Institute (HL116186).

Duality of Interest. No potential conflicts of interest relevant to this article were reported.

Author Contributions. J.H. carried out most of the experiments, analyzed data, and wrote the manuscript. B.E.S., C.R.H., Y.T., and B.W. carried out experiments and analyzed data. M.W. conducted BMT experiments and analyzed data. J.R. performed bariatric surgeries, provided tissue samples, and supervised all clinical studies. A.B. and B.G.H. reviewed results, contributed to the planning of the project, and wrote the manuscript. M.S. planned and supervised the project, analyzed and interpreted data, and wrote the manuscript. M.S. is the guarantor of this work and, as such, had full access to all the data in the study and takes responsibility for the integrity of the data and the accuracy of the data analysis.

References

1. Gregor MF, Hotamisligil GS. Inflammatory mechanisms in obesity. Annu Rev Immunol 2011;29:415–445

2. Nathan C, Ding A. Nonresolving inflammation. Cell 2010;140:871–882

3. Talukdar S, Oh Y, Bandyopadhyay G, et al. Neutrophils mediate insulin resistance in mice fed a high-fat diet through secreted elastase. Nat Med 2012; 18:1407–1412

4. Winer DA, Winer S, Shen L, et al. B cells promote insulin resistance through modulation of T cells and production of pathogenic IgG antibodies. Nat Med 2011; 17:610–617

5. Weisberg SP, McCann D, Desai M, Rosenbaum M, Leibel RL, Ferrante AW Jr. Obesity is associated with macrophage accumulation in adipose tissue. J Clin Invest 2003;112:1796–1808

6. Nishimura S, Manabe I, Nagasaki M, et al. CD8+ effector T cells contribute to macrophage recruitment and adipose tissue inflammation in obesity. Nat Med 2009;15:914–920

7. DeFuria J, Belkina AC, Jagannathan-Bogdan M, et al. B cells promote inflammation in obesity and type 2 diabetes through regulation of T-cell function and an inflammatory cytokine profile. Proc Natl Acad Sci U S A 2013;110:5133–5138

8. Spite M, Clària J, Serhan CN. Resolvins, specialized proresolving lipid mediators, and their potential roles in metabolic diseases. Cell Metab 2014;19: 21–36

9. Serhan CN, Brain SD, Buckley CD, et al. Resolution of inflammation: state of the art, definitions and terms. FASEB J 2007;21:325–332

10. De Taeye BM, Novitskaya T, McGuinness OP, et al. Macrophage TNF-alpha contributes to insulin resistance and hepatic steatosis in diet-induced obesity. Am J Physiol Endocrinol Metab 2007;293:E713–E725

11. Uysal KT, Wiesbrock SM, Marino MW, Hotamisligil GS. Protection from obesity-induced insulin resistance in mice lacking TNF-alpha function. Nature 1997;389:610–614

12. Cho KW, Morris DL, DelProposto JL, et al. An MHC II–dependent activation loop between adipose tissue macrophages and CD4+ T cells controls obesity-induced inflammation. Cell Reports 2014;9:605–617

13. Morris DL, Cho KW, Delproposto JL, et al. Adipose tissue macrophages function as antigen-presenting cells and regulate adipose tissue CD4+ T cells in mice. Diabetes 2013;62:2762–2772

14. Moraes-Vieira PM, Yore MM, Dwyer PM, Syed I, Aryal P, Kahn BB. RBP4 activates antigen-presenting cells, leading to adipose tissue inflammation and systemic insulin resistance. Cell Metab 2014;19:512–526

15. Arai S, Maehara N, Iwamura Y, et al. Obesity-associated autoantibody production requires AIM to retain the immunoglobulin M immune complex on follicular dendritic cells. Cell Reports 2013;3:1187–1198

16. Wentworth JM, Naselli G, Brown WA, et al. Pro-inflammatory CD11c+CD206+ adipose tissue macrophages are associated with insulin resistance in human obesity. Diabetes 2010;59:1648–1656

17. Xu X, Grijalva A, Skowronski A, van Eijk M, Serlie MJ, Ferrante AW Jr. Obesity activates a program of lysosomal-dependent lipid metabolism in adipose tissue macrophages independently of classic activation. Cell Metab 2013;18: 816–830

18. Zeyda M, Gollinger K, Kriehuber E, Kiefer FW, Neuhofer A, Stulnig TM. Newly identified adipose tissue macrophage populations in obesity with distinct chemokine and chemokine receptor expression. Int J Obes 2010;34:1684–1694

19. Lee HS, Park JH, Kang JH, Kawada T, Yu R, Han IS. Chemokine and chemokine receptor gene expression in the mesenteric adipose tissue of KKAy mice. Cytokine 2009;46:160–165

20. Förster R, Davalos-Misslitz AC, Rot A. CCR7 and its ligands: balancing immunity and tolerance. Nat Rev Immunol 2008;8:362–371

21. Förster R, Schubel A, Breitfeld D, et al. CCR7 coordinates the primary immune response by establishing functional microenvironments in secondary lymphoid organs. Cell 1999;99:23–33

22. Chen Y, Tian Y, Ji Z, Liu Z, Shang D. CC-chemokine receptor 7 is overexpressed and correlates with growth and metastasis in prostate cancer. Tumour Biol 2015;36:5537–5541

23. Tutunea-Fatan E, Majumder M, Xin X, Lala PK. The role of CCL21/CCR7 chemokine axis in breast cancer-induced lymphangiogenesis. Mol Cancer 2015;14:35

24. Cuesta-Mateos C, Loscertales J, Kreutzman A, et al. Preclinical activity of anti-CCR7 immunotherapy in patients with high-risk chronic lymphocytic leukemia. Cancer Immunol Immunother 2015;64:665–676

25. Damås JK, Smith C, Øie E, et al. Enhanced expression of the homeostatic chemokines CCL19 and CCL21 in clinical and experimental atherosclerosis: possible pathogenic role in plaque destabilization. Arterioscler Thromb Vasc Biol 2007;27:614–620

26. Halvorsen B, Dahl TB, Smedbakken LM, et al. Increased levels of CCR7 ligands in carotid atherosclerosis: different effects in macrophages and smooth muscle cells. Cardiovasc Res 2014;102:148–156
27. Spite M, Hellmann J, Tang Y, et al. Deficiency of the leukotriene B4 receptor, BLT-1, protects against systemic insulin resistance in diet-induced obesity. J Immunol 2011;187:1942–1949
28. Kroon E, Martinson LA, Kadoya K, et al. Pancreatic endoderm derived from human embryonic stem cells generates glucose-responsive insulin-secreting cells in vivo. Nat Biotechnol 2008;26:443–452
29. Kodati S, Chauhan SK, Chen Y, et al. CCR7 is critical for the induction and maintenance of Th17 immunity in dry eye disease. Invest Ophthalmol Vis Sci 2014;55:5871–5877
30. Alfonso-Pérez M, López-Giral S, Quintana NE, Loscertales J, Martín-Jiménez P, Muñoz C. Anti-CCR7 monoclonal antibodies as a novel tool for the treatment of chronic lymphocyte leukemia. J Leukoc Biol 2006;79:1157–1165
31. Gautier EL, Shay T, Miller J, et al.; Immunological Genome Consortium. Gene-expression profiles and transcriptional regulatory pathways that underlie the identity and diversity of mouse tissue macrophages. Nat Immunol 2012;13:1118–1128
32. Martinez-Santibañez G, Lumeng CN. Macrophages and the regulation of adipose tissue remodeling. Annu Rev Nutr 2014;34:57–76
33. Bertola A, Ciucci T, Rousseau D, et al. Identification of adipose tissue dendritic cells correlated with obesity-associated insulin-resistance and inducing Th17 responses in mice and patients. Diabetes 2012;61:2238–2247
34. Schwab JM, Chiang N, Arita M, Serhan CN. Resolvin E1 and protectin D1 activate inflammation-resolution programmes. Nature 2007;447:869–874
35. Kuan EL, Ivanov S, Bridenbaugh EA, et al. Collecting lymphatic vessel permeability facilitates adipose tissue inflammation and distribution of antigen to lymph node-homing adipose tissue dendritic cells. J Immunol 2015;194:5200–5210
36. Xu H, Hertzel AV, Steen KA, Wang Q, Suttles J, Bernlohr DA. Uncoupling lipid metabolism from inflammation through fatty acid binding protein-dependent expression of UCP2. Mol Cell Biol 2015;35:1055–1065
37. Sano T, Iwashita M, Nagayasu S, et al. Protection from diet-induced obesity and insulin resistance in mice lacking CCL19-CCR7 signaling. Obesity (Silver Spring) 2015;23:1460–1471
38. Luchtefeld M, Grothusen C, Gagalick A, et al. Chemokine receptor 7 knockout attenuates atherosclerotic plaque development. Circulation 2010;122:1621–1628
39. Harvey NL, Srinivasan RS, Dillard ME, et al. Lymphatic vascular defects promoted by Prox1 haploinsufficiency cause adult-onset obesity. Nat Genet 2005;37:1072–1081
40. Pond CM, Mattacks CA. In vivo evidence for the involvement of the adipose tissue surrounding lymph nodes in immune responses. Immunol Lett 1998;63:159–167
41. Scallan JP, Hill MA, Davis MJ. Lymphatic vascular integrity is disrupted in type 2 diabetes due to impaired nitric oxide signalling. Cardiovasc Res 2015;107:89–97
42. Souza SC, Palmer HJ, Kang YH, et al. TNF-alpha induction of lipolysis is mediated through activation of the extracellular signal related kinase pathway in 3T3-L1 adipocytes. J Cell Biochem 2003;89:1077–1086
43. Kosteli A, Sugaru E, Haemmerle G, et al. Weight loss and lipolysis promote a dynamic immune response in murine adipose tissue. J Clin Invest 2010;120:3466–3479
44. Fonseca DM, Hand TW, Han SJ, et al. Microbiota-dependent sequelae of acute infection compromise tissue-specific immunity. Cell 2015;163:354–366